Synthesis and characterization of low work function alkali oxide thin films for unconventional thermionic energy converters

Valentina Giorgis, François Morini, Tianqi Zhu, J.F. Robillard, X. Wallart, Jean-Louis Codron, Emmanuel Dubois

Journal of Applied Physics

Synthesis and characterization of low work function alkali oxide thin films for unconventional thermionic energy converters

Cite as: J. Appl. Phys. **120**, 205108 (2016); https://doi.org/10.1063/1.4968532
Submitted: 24 May 2016 • Accepted: 17 October 2016 • Published Online: 30 November 2016

V. Giorgis, F. Morini, T. Zhu, et al.

JOURNAL OF APPLIED PHYSICS **120**, 205108 (2016)

Synthesis and characterization of low work function alkali oxide thin films for unconventional thermionic energy converters

V. Giorgis,[1,a)] F. Morini,[2] T. Zhu,[1] J.-F. Robillard,[1] X. Wallart,[1] J.-L. Codron,[1] and E. Dubois[1]
[1]*Institut d'Electronique, de Microélectronique et des Nanotechnologies (IEMN), UMR CNRS 8520, Cité Scientifique, Avenue Poincaré, BP 60069, 59652 Villeneuve d'Ascq Cedex, France*
[2]*GREMAN UMR CNRS 7347 16, rue Pierre et Marie Curie, 37071 Tours, France*

(Received 24 May 2016; accepted 17 October 2016; published online 30 November 2016)

In this work, we present the synthesis and the characterization of low work function thin films for Micro Thermionic Converters (MTC). The objective is producing a device operating at relatively low temperature (<1000 K). We aim at improving the MTC efficiency by reducing the work function of the electrodes and increasing the emitted current density by alkali metal oxides electrodes coating. In particular, in this work, we analyse and compare the performances of two alkali metal oxides: potassium and caesium oxides. Our choice to exploit those materials relies on their low work function and their abundance. For both materials, we present the results on the synthesis of the oxides under high vacuum and controlled temperature. The oxide thin films were characterized by X-ray photoelectron spectroscopy, photoemission, and thermionic emission measurements. By exploiting the latter technique, a quantitative evaluation of the current density, emitted by the heated oxides, is obtained as a function of temperature. Our results demonstrate that it is possible to decrease the silicon work function by almost 3 eV, enabling significant thermionic currents despite relatively low temperatures (below 850 K). *Published by AIP Publishing.*
[http://dx.doi.org/10.1063/1.4968532]

I. INTRODUCTION

The idea of directly converting heat into electricity is attracting the scientific community, since at least the beginning of the twentieth century, when Schlichter first proposed a heat engine based on thermionic emission.[1] One of the earliest layout of the Thermionic Converter (TC) consisted in two parallel electrodes separated by a macrometric gap (>100 μm).[2] In this original device, the emitting electrode, held at a high temperature (typically 1800–2000 K), emits electrons through the gap to the cold electrode, the collector, held at lower temperature (900–1000 K). To be injected in the gap, the electrons energy should overcome the electrode's work function. The efficiency of this device, in principle very high in the ideal case, is limited in practice by the heat losses and the consistent space charge build-up in the macrometric gap. Ionized gases, in particular, caesium vapour, were employed to neutralize the space charge, but the formed plasma requires high temperatures (2000 K) to be maintained.[3] Therefore, the idea of using the TCs to convert heat into electrical energy was gradually abandoned, due to the high costs of the traditional thermionic converters and the technical issues. Recently, however, the interest in the parallel electrodes design has been renewed,[4,5] thanks to the advances in fabrication technology made in the last decades, too. Exploiting the processes optimized for the fabrication of MEMS (Microelectromechanical systems) and NEMS (Nanoelectromechanical systems), it is now possible to produce Micro Thermionic Converters (MTC hereafter), and having the electrode pair separated by a micrometric (<10 μm) vacuum gap, a distance comparable with the electrons mean free path, enabling a ballistic charge transfer between the electrodes and reducing the space charge (Figure 1). Thus, the improvement of the performance of the device relies essentially on the minimization of the work function of the electrodes and on the optimization of the gap width.

This work aims at the optimization of the electrode's coating film characteristics in terms of lowering the electrodes work function and increasing the produced electronic current. Our scope is the development of MTC operating at low temperatures for low power applications.

The thermionic current density is given by Richardson's equation

$$J = A^* A_0 T^2 \exp\left(-\frac{\phi + qV}{kT}\right), \tag{1}$$

where A^* is the specific correction factor that depends on the material, A_0 is the Richardson constant (120 A/cm^2 K^2), ϕ is the material work function, V is the voltage between the electrodes, and T is the temperature of the emitter.

We propose potassium and caesium oxides as silicon electrode coating to reduce the electrode's work function. It is well known that both elements present very low work functions,[6] and it has been shown[7–13] that they can decrease the work function of the substrate they are adsorbed on. This paper reports the results on the synthesis and characterization of the two alkali metal oxides. Our approach allows to achieve low sample work function (<2 eV), relatively high thermionic current densities (up to 12.8 μA/cm^2) at low temperature (<800 K), representing an improvement toward efficient MTC.[5,14]

[a)]valentina.giorgis@isen.iemn.univ-lille1.fr

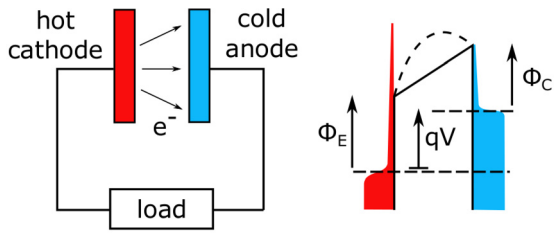

FIG. 1. Left: electric scheme of the MTC. The transport of the thermoemitted electrons is ballistic. Right: energy diagram across the vacuum gap. ϕ_E and ϕ_C are the work functions, respectively, of the hot emitter and the cold collector, $q = -e$ is the electron charge, V is the voltage difference between the two electrodes. The interelectrode potential is represented by a solid line in the ideal case and by a dashed line when the space charge effect is taken into account.

II. DEPOSITION SET-UP, SAMPLE PREPARATION, AND MEASUREMENT METHODOLOGY

In our study, we took advantage of a dedicated measurement set-up, which permits to deposit and characterize the alkali oxide thin film *in situ*. The alkali oxides are deposited by resistive evaporation on silicon (100) substrates (p-type Boron doped, resistivity 5–10 Ω cm). The samples characteristics, i.e., work function and emitted current density, are analysed by photoemission and thermionic emission measurements. The composition of the thin films is investigated by X-ray Photoelectron Spectroscopy (XPS). The set-up is depicted in Figure 2: it consists of a UHV chamber, which includes a resistive evaporation facility, a Kelvin probe, an optical entry for photoemission measurements, and a radiative heater included in the sample holder. The oxygen is introduced in the chamber by means of a leakage valve. Photoemission and thermionic emission measurements are performed by coupling the Kelvin probe (by KP Technology) with, respectively, the optical system and the sample heating system. In thermionic emission measurements, the electrons emitted by the sample and collected by the tip of the Kelvin probe. Thus, the sample acts as an emitter of MTC, the tip of the probe as the collector, having $\phi_E = \phi_{SAMPLE}$ and $\phi_C = \phi_{TIP}$. However, the work function of the tip, $\phi_{TIP} = 4.764$ eV,[15] is too high for a collector to be used in a operative MTC.

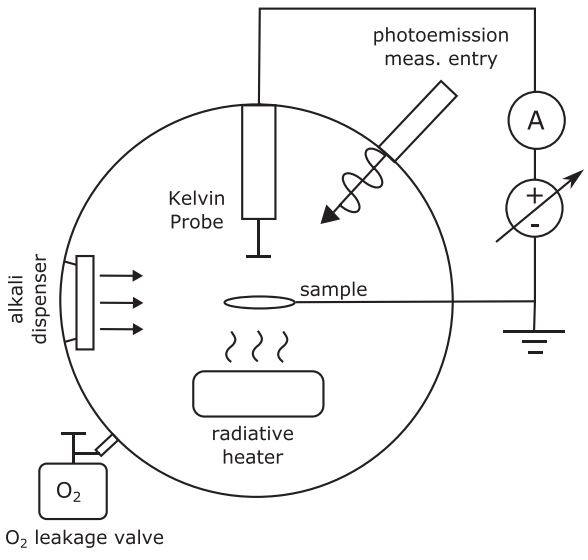

FIG. 2. Schematic of the set-up.

The silicon substrate is cleaned before the oxide deposition. The substrate is immersed first in piranha solution (H_2SO_4:H_2O_2/1:1, in volume) for 10 min, to remove organic contaminants and to oxidise the surface, then in hydrofluoric acid (HF 5%) to remove the native oxide. After the process, the silicon surface is H-terminated.[16] Potassium and caesium are then deposited on the H-Si substrate at room temperature, under an oxygen atmosphere.[17] The alkali is released by resistive evaporation by applying a 7.5 A current intensity to a dispenser (by SAES Group). The deposition time is 10 min. For both materials, the pressure is set at 4×10^{-7} mbar during the evaporation and held constant. A preliminary study to determine the optimal synthesis condition has been previously performed by our group.[7] Photoemission and thermionic emission measurements are performed under a base pressure of 3×10^{-9} mbar. In photoemission measurement, the sample is shone with monochromatic light and the photocurrent I_{ph} is harvested by the Kelvin probe, held at 1.5 cm from the sample. A potential bias V_b, which can vary from −10 V to +10 V, is applied to the Kelvin probe tip, in order to shift the tip Fermi level with respect to the sample one of a quantity qV_b (Figure 3(a)). The photoemission measurements allow to extrapolate the work function of both the sample and the Kelvin probe tip. In the sample work function (ϕ_{SAMPLE}) measurement, V_b is set at +10 V and the sample can be illuminated in the 1.7–3.0 eV range. It is possible to extract ϕ_{SAMPLE} from the plot of cubic root of I_{ph} versus the incident photon energy $h\nu$,[18] given that the sample is a semiconductor[19]

$$\sqrt[3]{I_{ph}} \propto (h\nu - \phi_{SAMPLE}). \tag{2}$$

As stated previously, the tip probe work function, ϕ_{TIP}, can be measured, too, by photoemission. To extrapolate ϕ_{TIP}, we proceed by measuring the square root of photocurrent, $\sqrt{I_{ph}}$, as a function of V_b for given wavelengths. The highest V_b value at which $\sqrt{I_{ph}}$ is null is the cut-off potential V_0, which can be extracted by fitting the obtained curves. At V_0, $h\nu = \phi_{TIP} + qV_0$; therefore, ϕ_{TIP} can be extrapolated from the plot of V_0 versus the incident photon energy.

The thermionic emission measurements are performed by heating the sample, from 500 K to 800 K, and harvesting the produced thermocurrent by applying to the probe tip $V_b = +10$ V (Figure 4(a)). As in photoemission measurements, the tip is held 1.5 cm above the sample's surface. From the plot of current density J as a function of the temperature T, it is possible to obtain the maximum current density. The sample work function is extrapolated from the same data, arranged in an Arrhenius plot of J.

The composition of the film was investigated by XPS measurements, right after the film deposition and after the sample annealing caused by the heating procedure in thermionic emission measurements, in order to study the potential changes in the film composition.

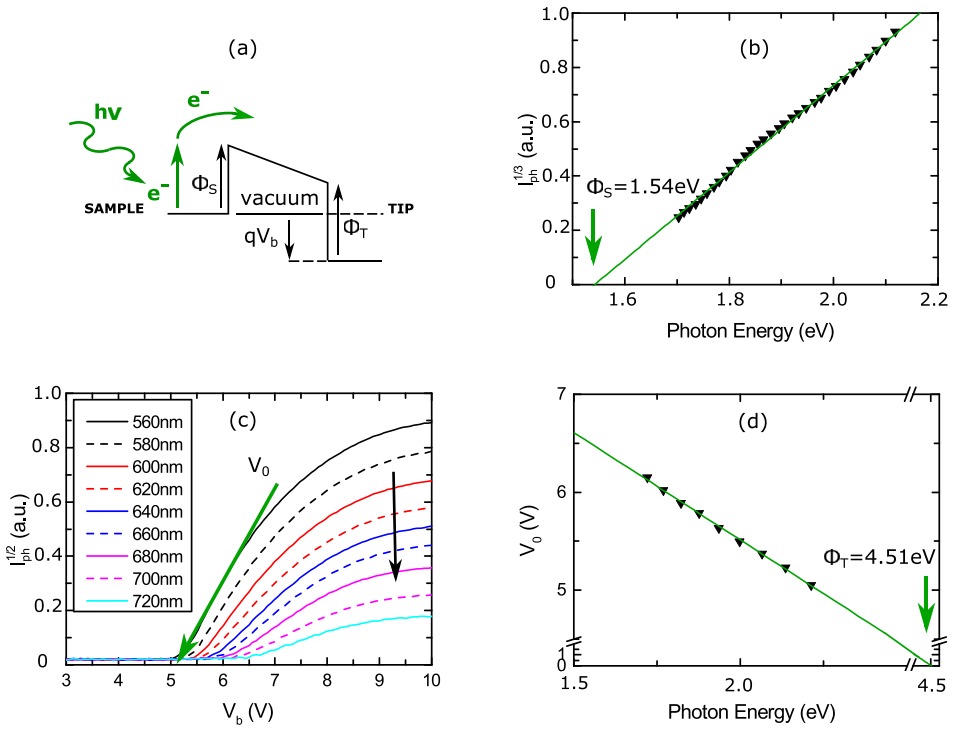

FIG. 3. (a) Energy band diagram of photonic emission. (b) Potassium oxide experiment. Plot of the cubic root of photocurrent, $\sqrt[3]{I_{ph}}$, as a function of the incident photon energy $h\nu$. (c) Tip work function extrapolation. Plot of square root if photocurrent, $\sqrt{I_{ph}}$ as a function of V_b, for given wavelengths. (d) Tip work function extrapolation. Plot of the cut-off voltage V_0 as a function of $h\nu$ and ϕ_{TIP} extrapolation.

III. RESULTS

In the following sections, we describe in detail the measurement procedures for extracting the work function of Kelvin probe tip (Section III A) and sample, for both potassium (Section III B) and caesium (Section III C), and the XPS analysis on the alkali oxides thin films (Section III D). A typical example is discussed for work function extraction analyses, and then, the general results are given.

A. Tip work function

The tip work function was measured by photoemission. In Figures 3(c) and 3(d), we report a typical example of the analysis. The square root of the photocurrent was collected by the Kelvin probe as the voltage V_b varied from +3 V to +10 V, while the sample was illuminated by monochromatic light in the range $\lambda = 560{:}720$ nm. The intercept of the linear fit of the slopes of the I–V curves and the x-axis gave the values of V_0, then plotted in Figure 3(d) as a function of $h\nu$. The intercept of the line fitting V_0 points and the energy axis gave $\phi_{TIP} = 4.51$ eV. The measurement was performed 10 times during various deposition campaign at different experiment stages, obtaining a mean value for $\phi_{TIP} = 4.39 \pm 0.62$ eV. This value is comparable with the value $\phi_{TIP} = 4.764$ eV, given by the Kelvin probe manufacturer.[15]

B. Potassium

Potassium deposition and characterization were performed on seven different samples.

We show in Figure 3(b) an example of photoemission analysis. The value of the sample work function, evaluated from the plot of $\sqrt[3]{I_{ph}}$ as a function of photon energy, is 1.54 eV, while bare silicon surface work function is in the 4.1–5.3 eV range. The thermionic emission measurements were performed heating the sample from 500 K to the maximum temperature 805 K. The analysis is shown in Figures 4(b) and 4(c). From the first plot (Figure 4(b)), J versus T, it is possible to extract the information about the evolution of the thermocurrent density: it starts increasing around $T = 750$ K, and reaches 2.4 μA/cm^2 at 805 K, the highest temperature in this experiment. To extrapolate ϕ_{SAMPLE} from the Arrhenius plot (Figure 4(c)), we fitted the region where the current density dramatically increases with the temperature, from 750 K to 805 K, obtaining $\phi_{SAMPLE} = 1.92$ eV. The values extracted from the Arrhenius plot were used for the curve in the form of Richardson's equation (solid line in Figure 4(b)) that reproduces the experimental data trend. The values of ϕ_{SAMPLE} extracted by the measurements on all the potassium coating experiments are 1.73 ± 0.16 eV, for photoemission experiments, and 1.75 ± 0.28 eV, for thermionic emission experiments. The results of photoemission and thermionic emission measurements are comparable. The maximum current density was 3.6 μA/cm^2 at 799 K, harvested by the Kelvin probe tip on a potassium oxide covered sample applying +10 V to the tip, at the highest temperature reached for that experiment.

C. Caesium

The caesium oxide thin film was prepared and characterized on 10 samples. In Figure 5, we report the photoemission analysis on one of the performed measurements, $\sqrt[3]{I_{ph}}$ versus $h\nu$. The extracted value for the sample work function is 1.36 eV. Figure 6 shows the plot of the current density versus the temperature (Figure 6(a)) and the current density Arrhenius plot (Figure 6(b)) for a typical sample. The sample work function is evaluated by analysing the latter plot: $\phi_{SAMPLE} = 1.81$ eV. The evolution of J is depicted in Figure

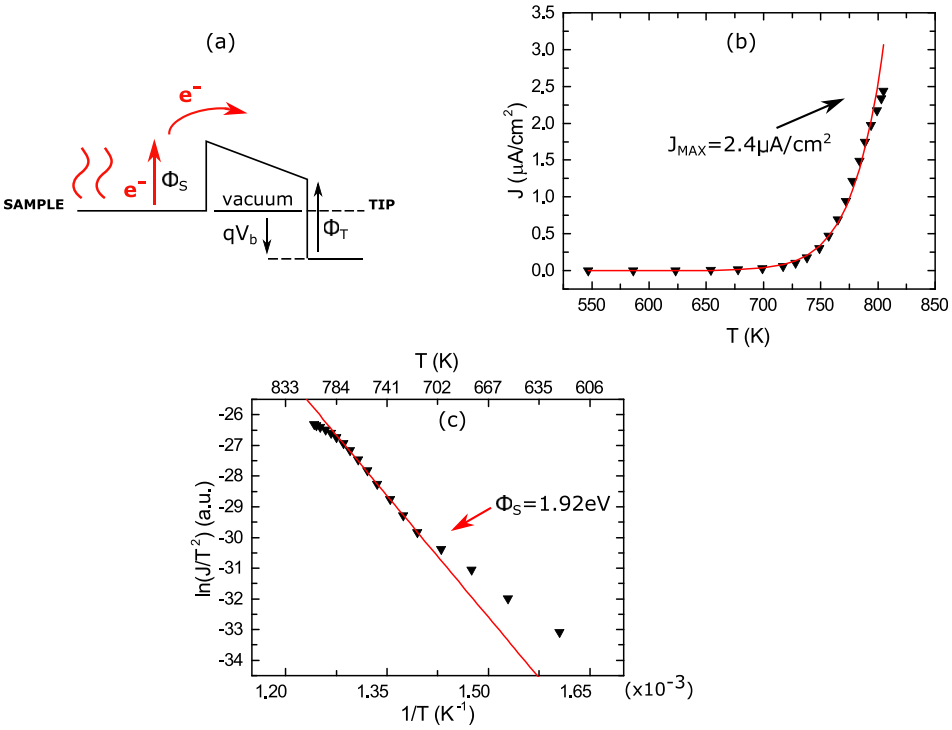

FIG. 4. (a) Energy band diagram of thermionic emission. (b) Potassium oxide experiment. Plot of thermionic current collected by the tip, biased at +10 V, as a function of the temperature, fitted with Richardson's equation, using values extracted from Arrhenius plot. (c) Potassium oxide experiment. Arrhenius plot.

6(a): the thermionic current density starts increasing at $T = 680$ K and reaches its maximum, 10 μA/cm^2, at 743 K. Again, the Richardson's curve (solid line in the same figure) reproduces the experimental data trend. It is worth noting that the caesium oxide cover sample presents a critical temperature, $T_C = 750$ K, above which the current density decreases. This behaviour was observed in each sample, with the critical temperature being between 700 K and 800 K. It is our opinion that the current drop is an indication of a modification in the film structure and composition.[20,21] All the samples which crossed their T_C, and later let cooling down, were not able to produce thermocurrent during a following measurement. This effect can be due to the modification in the film structure and composition or to the complete evaporation of the thin film at high temperatures (>1000 K) due to high volatility of Cs. To investigate the response of the film to annealing below T_C, we performed measurements heating the sample at three different temperatures: 700 K, 750 K, and 800 K. The sample was let cooling down before each temperature ramp. An example of this process is depicted in Figure 7: the sample was still emitting current if the temperature of the previous annealing did not exceed T_C. Concluding, the analyses performed on all the caesium oxide covered samples gave $\phi_{SAMPLE} = 1.66 \pm 0.27$ eV, for photoemission experiments, and $\phi_{SAMPLE} = 1.72 \pm 0.20$ eV, for thermionic emission experiments. The values are comparable. The highest achieved current density for these samples was 12.8 μA/cm^2 at 698 K.

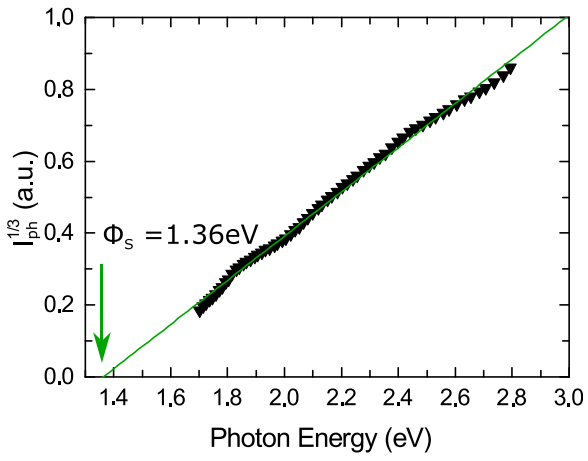

FIG. 5. Caesium oxide experiment. Plot of the cubic root of photocurrent as a function of the incident photon energy.

D. XPS measurements

XPS analysis was performed right after the oxide deposition and after the annealing due to thermionic emission measurement, both on potassium and caesium oxides covered samples.

XPS analyses were carried out using a Physical Electronics model 5600 system for which the base pressure is in the low 10^{-10} Torr range. A monochromatic Al Kα X-ray source making a 90° angle with the electrostatic hemispherical analyzer was used for all XPS measurements. The analyzer acceptance angle and pass energy were set to 14° and 12 eV, respectively. The analyzed area was 400 μm in diameter whereas the electron take-off angle was fixed to 45°. The collected XPS spectra were fitted by Gaussian-Lorentzian profiles, and the oxide composition was determined by standard quantitative analysis using the appropriate sensitivity factors.[22]

On potassium oxide covered samples, the oxide composition indicated a solid solution containing K_2O_2 and K_2O_3, both before and after the annealing. The result was further confirmed by the position of the O1s main peak at 532.05 eV, that we associated to the presence of potassium

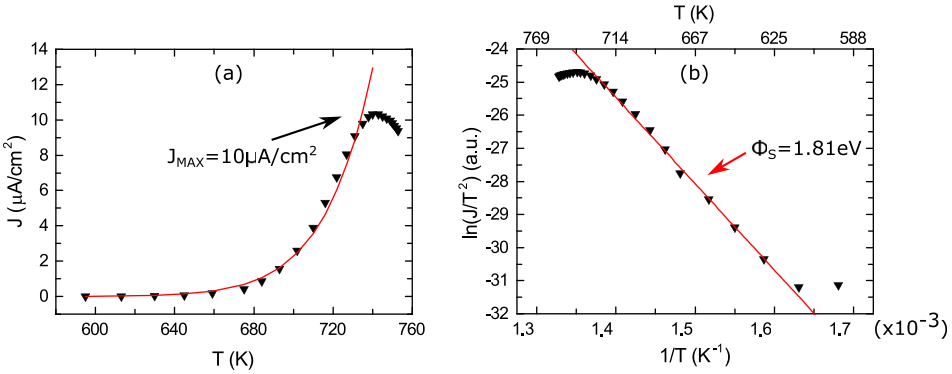

FIG. 6. Caesium oxide experiment. (a) Plot of thermionic current density as a function of the temperature, fitted with Richardson's equation, using values extracted from Arrhenius plot. (b) Arrhenius plot.

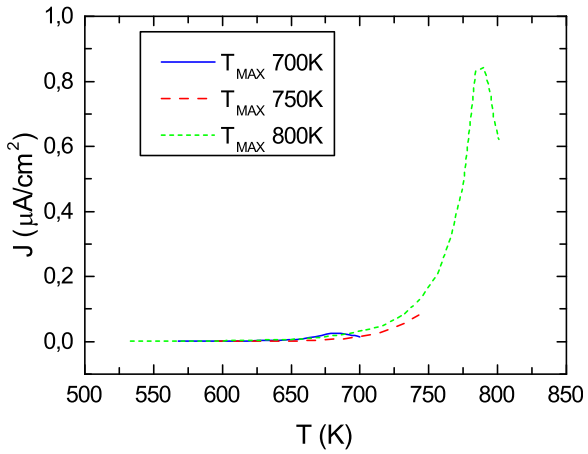

FIG. 7. Caesium oxide experiment. Plot of current density as a function of temperature. Measurements repeated, three temperature ramps: up to 700 K, 750 K, and 800 K. The sample cooled down between the measurements. When the temperature did not exceed the critical temperature, in this case 780 K, the sample emitted current during the successive measurements.

oxides,[10] and that remained unchanged before and after the annealing. We conclude that the annealing, up to 800 K, does not change the composition of the potassium oxide film.

On cesium oxide covered samples, XPS revealed a change in the sample composition after the annealing. Indeed CsO_2 is formed in the pre-annealing experiment, which is converted to Cs_2O_2 in the post-annealing experiment. The binding energy of the O1s peak associated with cesium oxide confirmed this finding, shifting from 531.74 eV (Ref. 23) to 532.45 eV before and after the annealing, respectively.

IV. DISCUSSION

A summary of the results obtained by photoemission and thermionic emission measurements is reported in Table I. The sample work functions extracted with the two techniques are comparable, for both potassium and caesium samples. Moreover, the extracted values are comparable for the two oxides.

TABLE I. Results of photoemission and thermionic emission experiments, for both potassium and caesium. The current density was collected applying +10 V to the Kelvin probe.

	ϕ_{PE} (eV)	ϕ_{TE} (eV)	J_{max} (μA/cm^2) @ T (K)
K/O:Si	1.73 ± 0.16	1.75 ± 0.28	3.6 @ 799
Cs/O:Si	1.66 ± 0.27	1.72 ± 0.20	12.8 @ 698

Another important result of the comparison of the two alkali oxides is depicted in Figure 8. Here, we compare the thermoemitted current density in potassium and caesium case (shown previously in Figures 4 and 6), collected by the tip of the Kelvin probe held at +10 V. The emitted current density is higher in the case of caesium, and its maximum value occurs at lower temperatures. Consequently, J starts increasing at lower temperatures: $T = 680$ K in the case of caesium, while for potassium, there is no significant thermionic signal below $T = 750$ K (Figure 8). It should be noted the presence, in the thermionic measurements on caesium samples, of a critical temperature T_c above which the current density decreases, possibly due to a change in the oxide film composition,[21] as evidenced by the XPS measurements. This behaviour was not present in potassium samples, for which we think the critical temperature is higher than our experimental temperature range.[20] Eventually, it should be noted that both the measurements methods present limitations: the measured work functions are outside the range of photon energy in photoemission measurements; the measured work functions are assumed to be independent from temperature in thermoemission measurements, and their extrapolation relies on approximations of Richardson-Dushman coefficient.

XPS measurements confirmed the presence of the same species of potassium oxides both before and after the annealing, supporting our intuition. Even though the presence of a

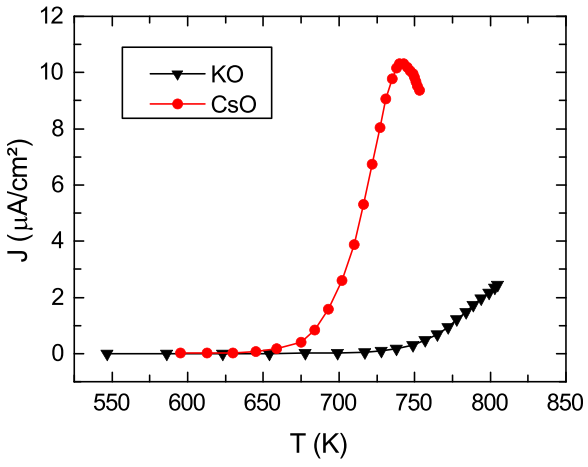

FIG. 8. Comparison between thermionic emission of caesium and potassium oxide.

relatively low critical temperature may be an issue for MTC design and applications, nonetheless caesium oxides samples performance are better compared to potassium in terms of emitted current density, in the range of temperature of interest (<1000 K).

V. PROSPECTS AND CONCLUSIONS

We compared the performance of potassium and caesium oxides film as low work function coating for MTC electrodes aiming at devices operating at low temperatures. We demonstrated that a low sample work function (<2 eV) can be achieved for both materials, having similar ϕ_{SAMPLE} values. Therefore, the silicon work function can be decreased by almost 3 eV. Moreover, we obtained significant thermionic currents at relatively low temperatures, applying low voltages to the probe/sample system. The XPS study performed on the coated samples was fundamental to demonstrate that caesium oxides composition changes above its critical temperature.

The comparison of the performances of potassium and caesium oxides brought to the conclusion that caesium oxides film is a preferred material for MTC electrodes coating. In the experimental temperature range, caesium oxides provide higher thermionic current at lower temperature, with maximum values of 12.8 μA/cm^2 at 698 K, with respect of potassium oxides film, 3.6 μA/cm^2 at 799 K.

ACKNOWLEDGMENTS

This work has been supported by the European Research Council under the European Community's Seventh Framework Programme (FP7/2007-2013) ERC Grant Agreement No. 338179, the French RENATECH network, and STMicroelectronics-IEMN Common Laboratory.

[1]W. Schlichter, Ann. Phys. **352**, 573 (1915).
[2]G. N. Hatsopoulos and J. Kaye, J. Appl. Phys. **29**, 1124 (1958).
[3]National Research Council, *Thermionics Quo Vadis? An Assessment of the DTRA's Advanced Thermionics Research and Development Program* (The National Academies Press, Washington, DC, 2001), pp. 1–70.
[4]D. B. King, K. R. Zavadil, D. R. Jennison, C. C. Battaile, and A. C. Marshall, "Low work function material development for the microminiature thermionic converter," Technical Report No. SAND2004-0555, Sandia National Laboratories (2004).
[5]J.-H. Lee, I. Bargatin, B. K. Vancil, T. O. Gwinn, R. Maboudian, N. A. Melosh, and R. T. Howe, J. Microelectromech. Syst. **23**, 1182 (2014).
[6]S. Sze, *Physics of Semiconductor Devices* (John Wiley & Sons, 1981).
[7]F. Morini, E. Dubois, J. F. Robillard, S. Monfray, and T. Skotnicki, Phys. Status Solidi (a) **211**, 1334 (2014).
[8]N. Rasor, Proc. IEEE **51**, 733 (1963).
[9]N. S. Rasor and C. Warner, J. Appl. Phys. **35**, 2589 (1964).
[10]J. Wu, M. Ma, H. Zheng, H. Yang, J. Zhu, and M. Ji, Phys. Rev. B **60**, 17102 (1999).
[11]J. Wu, F. Li, J. Zhu, Z. Wang, M. Ji, and M. Ma, J. Phys.: Condens. Matter **13**, 8725 (2001).
[12]M. Kamaratos and C. Papageorgopoulos, Surf. Sci. **219**, 317 (1989).
[13]C. Papageorgopoulos, M. Kamaratos, S. Kennou, and D. Vlachos, Surf. Sci. **277**, 273 (1992).
[14]J.-H. Lee, I. Bargatin, N. a. Melosh, and R. T. Howe, Appl. Phys. Lett. **100**, 173904 (2012).
[15]I. D. Baikie, A. C. Grain, J. Sutherland, and J. Law, Appl. Surf. Sci. **323**, 45 (2014).
[16]K. Huba, D. Krix, C. Meier, and H. Nienhaus, J. Vac. Sci. Technol. A **27**, 889 (2009).
[17]E. Bertel, F. P. Netzer, G. Rosina, and H. Saalfeld, Phys. Rev. B **39**, 6082 (1989).
[18]V. V. Afanas'ev and A. Stesmans, J. Appl. Phys. **102**, 081301 (2007).
[19]H. Sonnenberg, Appl. Phys. Lett. **14**, 289 (1969).
[20]H. Okamoto, J. Phase Equilib. **20**, 167 (1999).
[21]H. Okamoto, J. Phase Equilib. Diffus. **31**, 86 (2010).
[22]J. Moulder, W. Stickle, P. Sobol, and K. Bomben, *Handbook of X-Ray Photoelectron Spectroscopy* (Perkin Elmer Corporation, Physical Electronics Division, 1992).
[23]P. Dolle, P. Louis, and J. Jupille, Vacuum **41**, 174 (1990).